

Supplementary Information

Nanoscale pores introduced into paper via mesoporous silica coatings using sol-gel chemistry

*J. J. Mikolei, D. Richter, R. Pardehkhorrām, C. Helbrecht, S. Schabel, T. Meckel, M. Biesalski, M. Ceolin, A. Andrieu-Brunsen**

Mesoporous silica coating on paper-based materials

Cotton linter or eucalyptus sulfate paper sheets with a dimension of 2 x 6 cm are dipped into a sol-gel solution with a constant dip speed. After remaining in the coating solution, the samples are withdrawn with a constant withdrawal speed of 2 mms⁻¹.

The coating procedure is based on the EISA process^[32], which allows the formation of mesoporous thin ceramic films at surfaces. During the dip coating process of the paper sheet, the solvent ethanol evaporates, which is reported to induce the micelle formation and micelle arrangement upon reaching the critical micelle concentration (CMC) of the block-co-polymer mesopore template Pluronic® F127 (Figure S 1 paper coating).^[32] Simultaneously, the hydrolysis and condensation of the silica precursor TEOS proceeds which is further favored by increasing temperature.^[32] Synchronizing these assembly and silica formation processes is essential for a successful mesostructure formation. For planar substrates the dip-coating procedure based on the EISA process is well established and the critical steps as well as their interplay are already identified, for example, in the work of Brinker et al or Grosso et al. ^[32] After the dip-coating the freshly coated samples get aged for 1 h before they undergo a thermal post-treatment. The dip-coating procedure as well as the aging take place under norm conditions at a relative humidity of 50 (± 5) % and a temperature of 25 (± 1) °C. The samples subsequently undergo a thermal post-treatment with a final temperature of 130 °C. During the thermal post-treatment (Figure S 1, step II) the hydrolysis and condensation of the precursor TEOS continues and thus the stabilization of the silica structure as well as the connection between silica coating with the fiber surface occurs. ^[32] In previous work of our group solid-state NMR measurements show that a temperature treatment up to 130 °C is sufficient for completing the hydrolysis and condensation of TEOS to a stable silica network.^[27] Freshly deposited silica coatings can be removed by washing with ethanol while a stable integration of the silica coating is obtained.^[27] A higher temperature is not possible because of the combustion temperature of the cellulose fiber (Figure S 2 a). At a temperature of 130 °C the template Pluronic® F127 remains inside the silica coating. Therefore, the template needs to be chemically extracted after the thermal post-treatment using 0.01 M HCl in ethanol bath for 3 days. Treating the silica-paper hybrid material up to a final temperature of 500 °C the template can be removed but also the cellulose fiber material is destroyed. Only the mesoporous silica coating remains. ^[32] Figure S 1 schematically depicts the coating procedure followed by the thermal post-treatment and the chemical extraction.

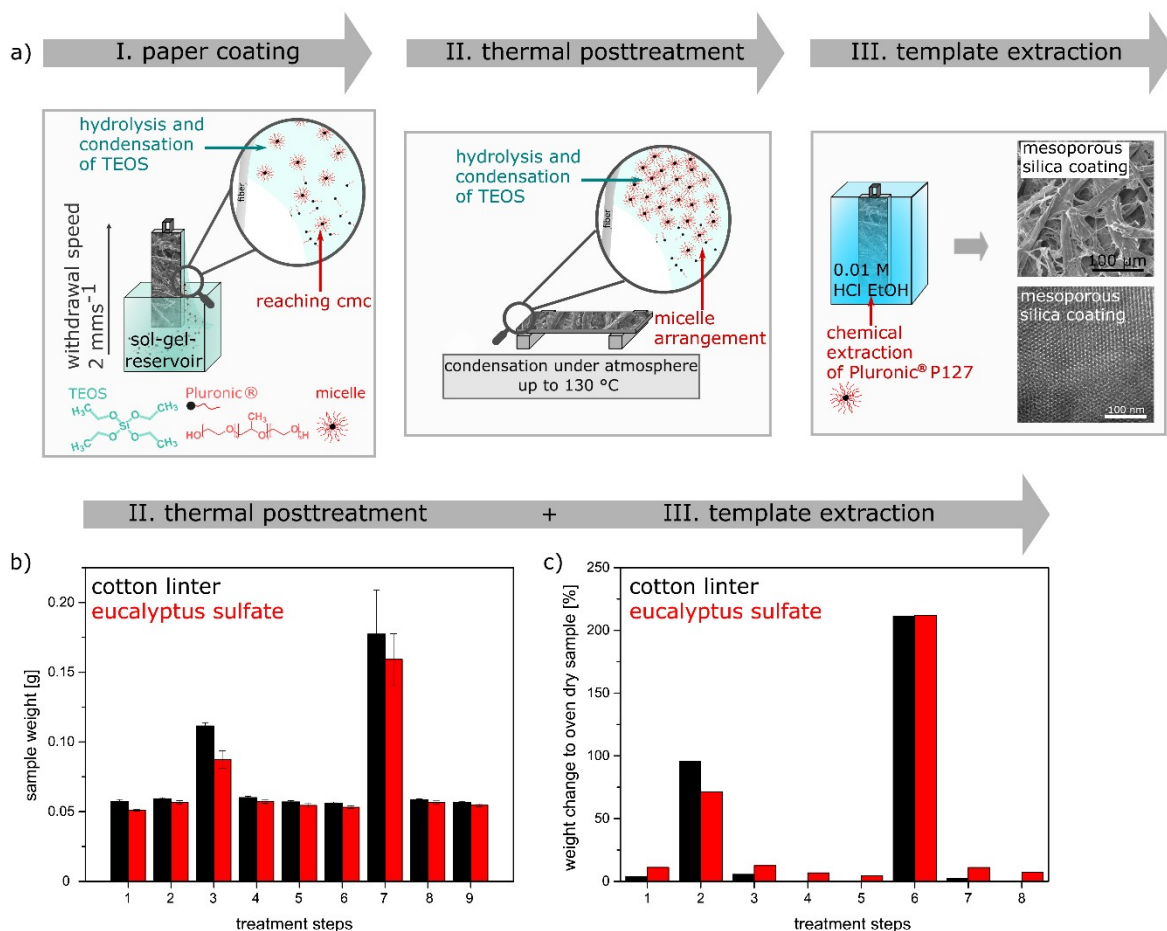


Figure S 1: a) Schematic illustration of the coating procedure to create a mesoporous silica coating on paper. b) and c) Change in the sample weight of cotton linters (black) and eucalyptus sulfate (red) paper due to the dipping into a ethanol solution followed by several drying steps (1 h at 25 °C, 1 h at 60 °C, 2 h at 130 °C), the ethanol extraction for 3 days followed again by drying at 25 °C for 24 h and at 80 °C for 12 h.

Change of the specific surface area and the mechanical properties of mesoporous silica coated cotton linter paper depending on the different thermal post-treatment programs

Cotton linter paper sheets with a dimension of 2 x 6 cm and a grammage of 40 gm⁻² were dip-coated using a mesoporous sol-gel solution with a precursor solvent ratio of 1 : 20. After the coating step the samples undergo a thermal post-treatment. The thermal post-treatment induces first the condensation of the precursor and second the covalent binding between the silica coating and the fiber surface. To investigate these two factors on the specific surface area as well as the mechanical properties of the hybrid material six different target temperatures ($t_1 = 25$ °C, $t_2 = 60$ °C, $t_3 = 130$ °C, $t_4 = 200$ °C, $t_5 = 350$ °C and $t_6 = 500$ °C) for the thermal post-treatment were used. Therefore, the silica coated samples were placed into an oven after 1 h of aging at a relative humidity of 50 (\pm 5) % and a temperature of 25 (\pm 1) °C. The oven was heated up from room temperature to one of the six different target temperatures with a heating rate of 10 Kmin⁻¹. After the post-treatment the amount of the deposited silica coating (TGA) (Figure S 2), the change of the surface area (Kr-BET) of the hybrid material as well as the change of the structural abilities of the paper after the temperature treatment with the special focus on their robustness were analyzed.

Cotton linter paper sheets are an organic material which burns at a certain temperature. To adjust the temperature program of the thermal post-treatment a TGA measurement of unmodified cotton linter paper samples was performed. Therefore, the sample undergoes a thermal treatment from 25 °C to 600 °C with a heating rate of 10 Kmin⁻¹. Figure 6 shows the curve of the mass loss in wt% depending on the temperature in °C. Between 25 °C and 100 °C a slight mass loss is visible. This mass loss is ascribed to the evaporation of the adsorbed water in the paper. After this first mass loss no further mass loss up to 270 °C is observed. At 280 °C the second significant mass loss occurs which is followed by a third mass loss at a temperature of 360 °C. At the temperature of 500 °C the TGA curve the detected mass remains constant. At the second and the third mass loss at 280 and 360 °C, different organic parts of the fiber are thermally destroyed. As the second mass loss at 280 °C is more dominant than the third one at 360 °C, it can be deduced that in the temperature range of 280 °C to 360 °C most of the organic parts are burned. Because of these significant changes in the mass loss temperature curve of the unmodified cotton linter paper samples and the combustion temperature of 350 °C of the template Pluronic® F 127 which is responsible for the mesopore formation in the sol-gel coating, the six different target temperatures were selected.

With the increase of the target temperature the color of the paper sheet changes from white to dark brown to white and the intrinsic stability of the paper decreases. The white color and the flexibility of the paper remain in the coated paper hybrid material for the target temperatures t_1 to t_3 (Figure S 2 b – h). The color of the hybrid material changes from white to slightly yellow at the target temperature t_4 of 200 °C (Figure S 2 e and f). Next to the color change the material becomes more brittle which indicates a decrease in the flexibility of the fiber and with these in the mechanical strength of the paper. With a further increase of the temperature from t_4 200 °C to t_5 350 °C (the combustion temperature of the used template Pluronic® F 127) the color changed from yellow to dark brown (Figure S 2 g) and the hybrid samples lose their shape during the thermal post-treatment. The dark brown color of the material indicates starting destruction of the organic cellulose paper fiber. At 500 °C a white powder remains and no further mass loss is detectable. The final change in the color indicates the complete removal of the organic cellulose paper fibers from the hybrid material. Only the silica coating remains at this temperature. Because of that a mechanically fragile and brittle material remains (see Figure S 2 h).

Samples which were cured at the target temperature below the combustion temperature of the template Pluronic® F 127 (350 °C) undergo an extraction step after the thermal post-treatment. Therefore, the samples are placed in an acidic ethanol bath for 3 days. This is not the case for samples with the target temperature of t_4 to t_6 . For all the paper silica hybrid samples TGA measurements were performed to calculate the amount of deposited silica coating. The measurements were performed with the same temperature program which is mentioned above for the unmodified paper samples. In Figure S 2 a the results of the TGA measurements are summarized. Interestingly, for the hybrid materials which underwent the target temperatures t_1 to t_3 no silica residue was detectable. With increasing the temperature

to t_4 and t_5 an amount of 8 wt% for the deposited silica was calculated applying the following equation.

$$m_{\text{deposited silica}} = \text{mass loss}_{\text{unmodified paper}} - \text{mass loss}_{\text{hybrid material}} \quad (1)$$

A further increase to a silica coating amount of 37 wt% and 98 wt% was detected for the target temperature t_6 and t_7 .

In addition to the TGA measurements also 11-point Kr-BET measurements at 77 K were performed for all six samples. For the samples with the target temperatures t_1 to t_3 no increase compared to the unmodified cotton linter paper was detectable (Figure S 2 a). This is an indication for the removal of the coating during the extraction. The specific surface areas for the samples with the target temperature of t_4 and t_5 are $17 \text{ m}^2\text{g}^{-1}$. Compared to unmodified cotton linter paper, the specific surface areas for the hybrid material increase and the temperature difference of $70 \text{ }^\circ\text{C}$ does not play a role for the size of the surface area. Only a color change occurs and the mechanical stability of the hybrid material decreases when using the target temperature t_5 . A further increase of the specific surface area to $86 \text{ m}^2\text{g}^{-1}$ can be observed with a target temperature of $350 \text{ }^\circ\text{C}$. Due to the color of this sample and the TGA results, the increase of the surface can be related to a higher content of the silica coating compared to the paper amount. The highest specific surface area of $681 \text{ m}^2\text{g}^{-1}$ is detected for the sample with the target temperature of $500 \text{ }^\circ\text{C}$ (t_6). This specific surface area is related to the pure silica coating. At a temperature of $500 \text{ }^\circ\text{C}$ the organic fiber is completely combusted and only the silica coating remains. Because of the decrease in mechanical stability at a temperature of $200 \text{ }^\circ\text{C}$ (t_4) and above, as well as the absence of a covalent bond between the silica coating and the fiber at a temperature of $60 \text{ }^\circ\text{C}$ (t_2), the target temperature of $130 \text{ }^\circ\text{C}$ (t_3) was used for the coatings.

a) methode	pure cotton linter	$t_1=25^\circ\text{C}$	$t_2=60^\circ\text{C}$	$t_3=130^\circ\text{C}$	$t_4=200^\circ\text{C}$	$t_5=350^\circ\text{C}$	$t_6=500^\circ\text{C}$
SBET [m^2g^{-1}]	1	1	1	16	17	83;	655
MBET [m^2g^{-1}]	1.18; 0.9993	2; 0.9997	2; 0.9997	17; 0.9999	18; 0.9997	86; 0.9999	681; 0.9991
silica residue [wt%]	~ 0	~ 0	~ 0	8	8	37	~ 98







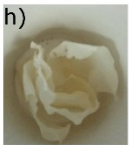


Figure S 2: Additional information to the TGA measurement in Figure 6. a) Table which summarizes the results for the Kr-BET measurements and the TGA measurements. b) – i) shows the images of the paper samples after the different temperature programs with the different target temperatures.

Fluid imbibition velocity in cotton linter and eucalyptus sulfate paper

The vertical fluid imbibition into unmodified eucalyptus sulfate and cotton linter differs in its velocity. For investigating the vertical fluid imbibition velocity, a eucalyptus sulfate and a cotton linter paper stripe of identical grammage are placed vertically into a fluid reservoir. After placing the paper samples into the fluid reservoir, the fluid imbibes into the paper sheet and is transported upwards caused by capillary forces (Figure S 3 a). After a certain time, the distance passed by the fluid is compared between the eucalyptus sulfate and cotton linter paper stripes (Figure S 3 b). In the same time period the fluid is transported a larger vertical distance along the cotton linter paper than in the eucalyptus sulfate paper.

To determine the vertical capillary fluid transport velocity in cotton linter (50 gm^{-2}) and eucalyptus sulfate (50 gm^{-2}) paper the fluid front of $100 \mu\text{L}$ distilled water was tracked and the time was plotted against distance (Figure S 3 c). The vertical capillary fluid transport velocity is based on the slope of the regression fit.

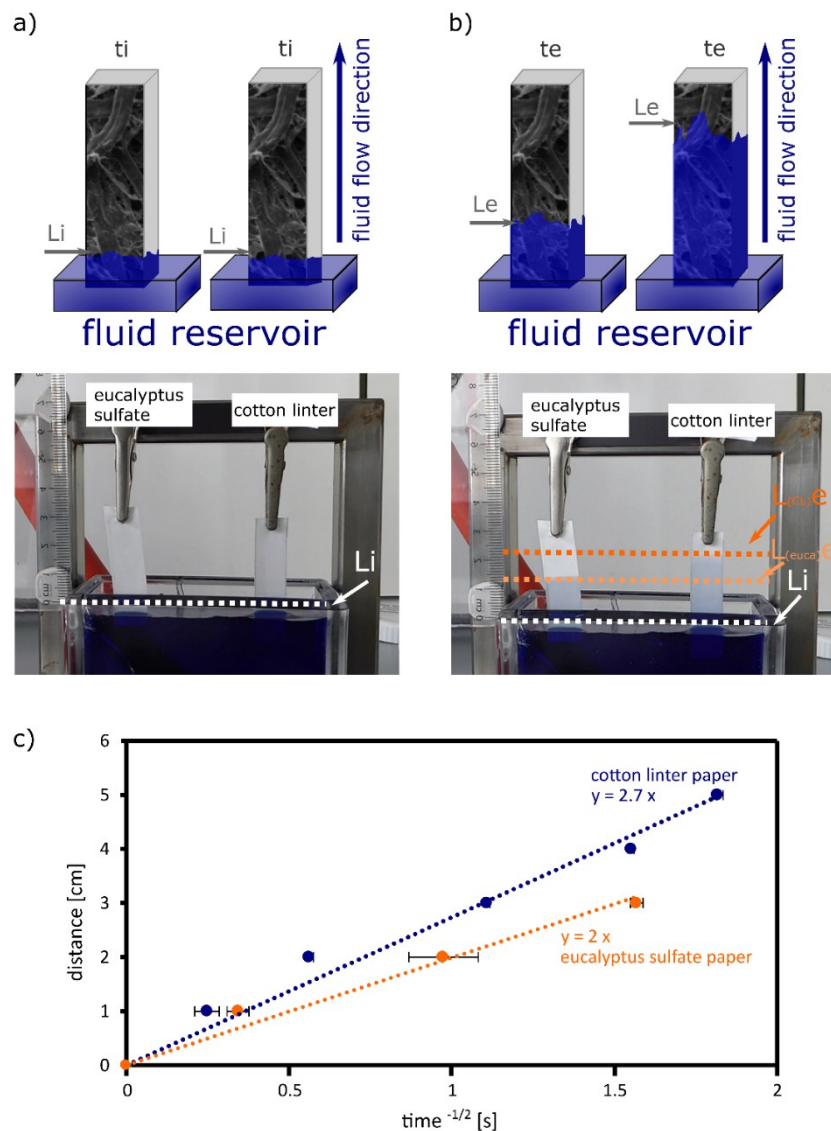


Figure S 3: a) Schematically description and a picture of the initial situation for the vertical fluid transport test at cotton linter and eucalyptus sulfate papers. b) The result of the vertical fluid transport test for cotton linter and eucalyptus sulfate papers described schematically and with a picture of the experiment. c) capillary water fluid flow measurement of un modified cotton linter (50 gm^{-2}) (blue) and eucalyptus sulphate (50 gm^{-2}) (orange) paper.

Pore formation during the dip coating process at silicon wafer

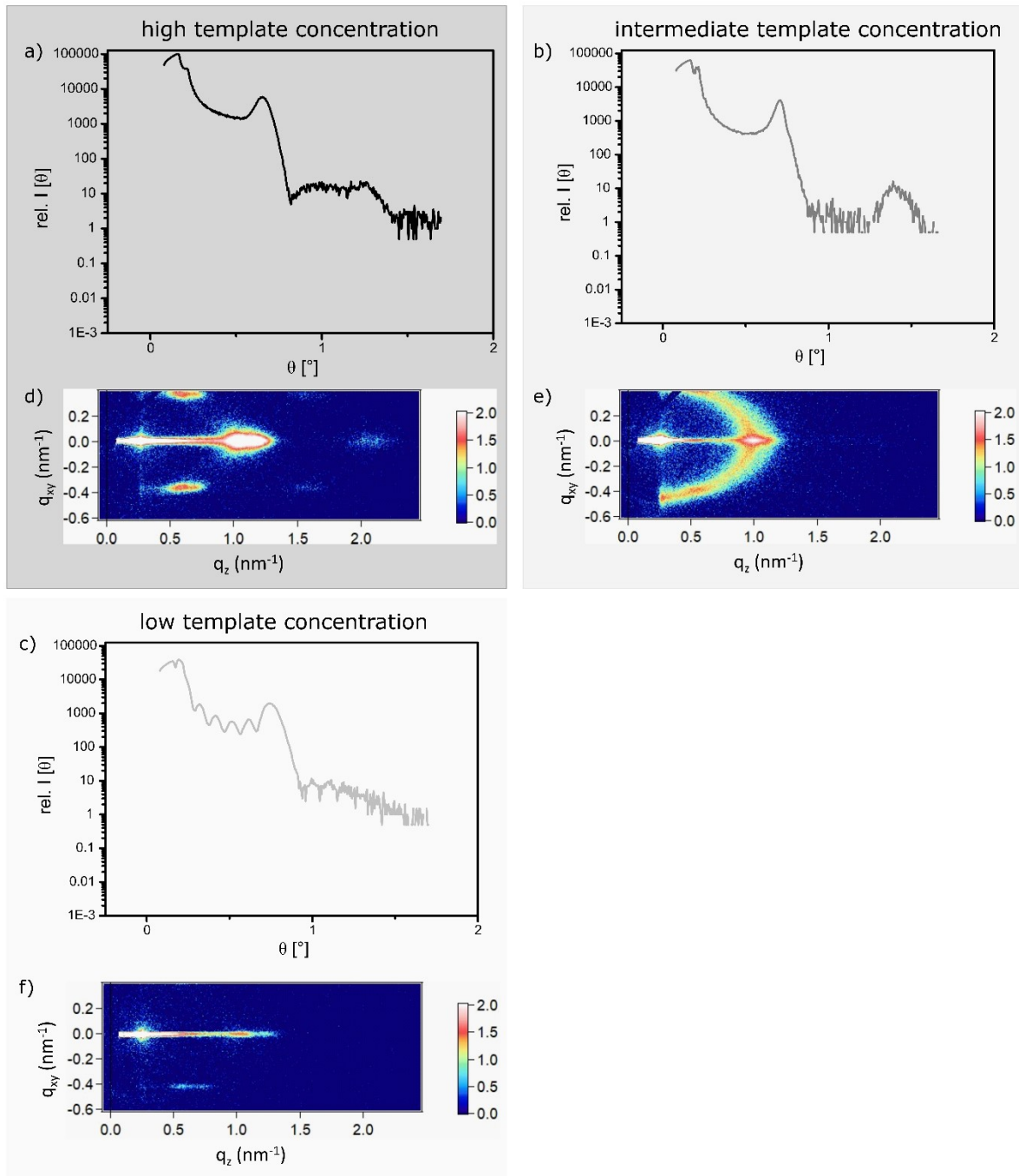


Figure S 4: a) – c) Results of the XRR experiments on silicon wafer coated with high (a), intermediate (b) and low (c) concentrated sol-gel solutions. d) – f) Results of the GISAXS experiments as well on silicon wafer coated with high (d), intermediate (e) and low template concentration.

Figure S 4 d) shows the GISAXS result of the silicon wafer coated with the high templated containing sol-gel solution. The GISAXS has spot pattern in the q_{xy} and q_z direction which is typical for vertical hexagonal ordered structure elements. In this case the pores in the coating of the silicon wafer are hexagonally orientated. A hexagonal ordered pore structure is also shown in the TEM images for the cotton linter papers which were coated with the high template containing sol-gel solution after the removal of the fibers at 500 °C (Figure 3 a). In the GISAXS for the silicon wafer coated with the intermediate template concentration the

spots start to vanish and instead of single spots one can see a semicircle characteristic for non-oriented samples (Figure S 4 e). But still the GISAXS prevails the orientation of the pores in a direction perpendicular to the substrate plane (xy). The spots in the GISAXS for the sample with the low template concentration the spots are completely vanished (Figure S 4 f). Only the main spot at the position $q_{xy}=0$ $q_z=1$, which is detected for all of the three samples, still remains. This indicates that the ordered structures have the same lattice spacing.

Table S 1: Summary of the critical angle (α_c), density (ρ), porosity, Bragg reflection (q)*, coating thickness (t), thickness of the single layers (D) and the number of the layers (n) extracted from the XRR spectra of silicon wafers coated with high, intermediate and low template concentrated sol-gel solution.

	α_c [°]	ρ [gcm ⁻³]	porosity [%]	q^* [nm ⁻¹]	Δq	t [nm]	D [nm]	n
1:20	0.164	1.92	33.8	0.92	-		6.8	
1:40	0.168	1.96	31.1	1	-		6.3	
1:80	0.157	1.83	40.4	1.05	0.14	45	6	7.5

$$\alpha_c = \sqrt{2\rho} \quad (2)$$

$$t = nD \quad (3)$$

$$q = \frac{4\pi}{\lambda} \sin \Theta \quad (4)$$

$$q^* = \frac{2\pi}{D} \quad (5)$$

$$\Delta q = \frac{2\pi}{t} \quad (6)$$

$$\text{porosity} = \frac{\rho_{SiO_2} - \rho_{sample}}{\rho_{SiO_2}} \quad (7)$$

with $\lambda = 0.15419$ nm

Determination of specific surface area, pore size and pore size distribution of mesoporous silica coating

The specific surface area of the silica-paper hybrid material is 16 m²g⁻¹ (Figure S 5 a) which is an increase of 13 times as compared to unmodified cotton linter paper with a specific surface area of 1.2 m²g⁻¹. The specific surface area is conducted with the Brunauer Emmett and Teller method (BET-method) in the relative pressure range from 0.05 to 0.3. There are two methods to obtain the specific surface area as well as the pore size and the pore size distribution of the “pure” silica coating without the paper. With one method, the sample amount at which the gas is adsorbed and desorbed is adjusted as described below. With the second method the paper material is thermally destroyed at 500 °C. At this temperature, only the silica coating remains from which the specific surface area can be determined directly via argon adsorption measurements. For the first method the sample amount of the hybrid material is adjusted via multiplication with coating amount which is obtained via TGA measurements (see equation 1). During the dip-coating with a sol-gel solution containing TEOS and ethanol in a 1 : 20 ratio, 8 wt% mesoporous silica is deposited at the cotton linter paper (see table in Figure S 2 b).

$$m_{\text{hybrid material}} * wt_{\text{silica residue}} = m_{\text{pure silica coating}} \quad (8)$$

In equation 9 this calculation is shown for one example. The sample mass of the gas adsorption experiment is mathematically reduced to the silica coating and is used in the evaluation software ASiQwin™ of Quantachrome.

$$0.138 \text{ g} * 8 * 10^{-2} \text{ wt\%} = 0.011 \text{ g} \quad (9)$$

Through this adjustment (reduction of the sample amount) there is no change in the isotherm shape compared to the isotherm of the silica-paper hybrid material and thus in the pore size and pore size distribution. There is only a change in the amount of adsorbed and desorbed gas (Figure S 5) which leads to a larger specific surface area of $206 \text{ m}^2\text{g}^{-1}$ (Figure S 5 b). This is a 13-fold relative increase which fits to the relative increase between the unmodified paper and the silica-paper hybrid material. With the second method a specific surface area of $305 \text{ m}^2\text{g}^{-1}$ is measured after thermal removal of the cotton linter cellulose paper fibers (Figure S 5 c). The specific surface area of mesoporous silica after paper destruction is thus 1.5 times higher than the mathematically determined from the hybrid material before cellulose paper fiber removal and 19 times higher than the unmodified cotton linter paper surface area. Specially, the differences in the relative increase between the specific surface area of the unmodified paper and the hybrid material as well as between the unmodified paper and the silica coating after thermal fiber removal shows a structural change in the silica coating upon cellulose paper fiber destruction. This is supported by comparing the isotherm shape as well as the pore size and pore size distribution of both materials. Argon adsorption measurements of silica coating obtained via the sample mass correction or combustion of the paper material show a type IV a) isotherm with a H 2 b) hysteresis loop which is typical for mesoporous materials (Figure S 5 b and c). The isotherm shape and the hysteresis loop are typical for mesoporous materials and proves that the mesopores remain in the coating during the paper combustion. Compared to the isotherm of the sample mass corrected one a higher amount of gas is adsorbed under a relative pressure of 0.5 which leads to a steeper increase of the isotherm. At relative pressures larger than 0.5 a smaller amount of gas is adsorbed. The differences in the isotherms are based on changes of the pore structures. The hybrid material and with this also the sample mass corrected values show the presence of micropores and mesopores with pore sizes of 2 nm and 5.7 nm with a narrow pore size distribution (Figure S 5 d). After the combustion the micropores with a diameter of 2 nm remain but in addition to the mesopores with a diameter of 5.7 nm mesopores with a diameter of 3.7 nm appear. The peak for the mesopores is broad and has a maximum at 3.7 nm and a shoulder at 5.7 nm. The pore size distribution shows that pores with a pore size of 3.7 nm are introduced into the silica coating during the thermal destruction of the cellulose paper fibers which indicates an imprinting of the fiber into the silica coating. The fiber gets templated during the silica coating.

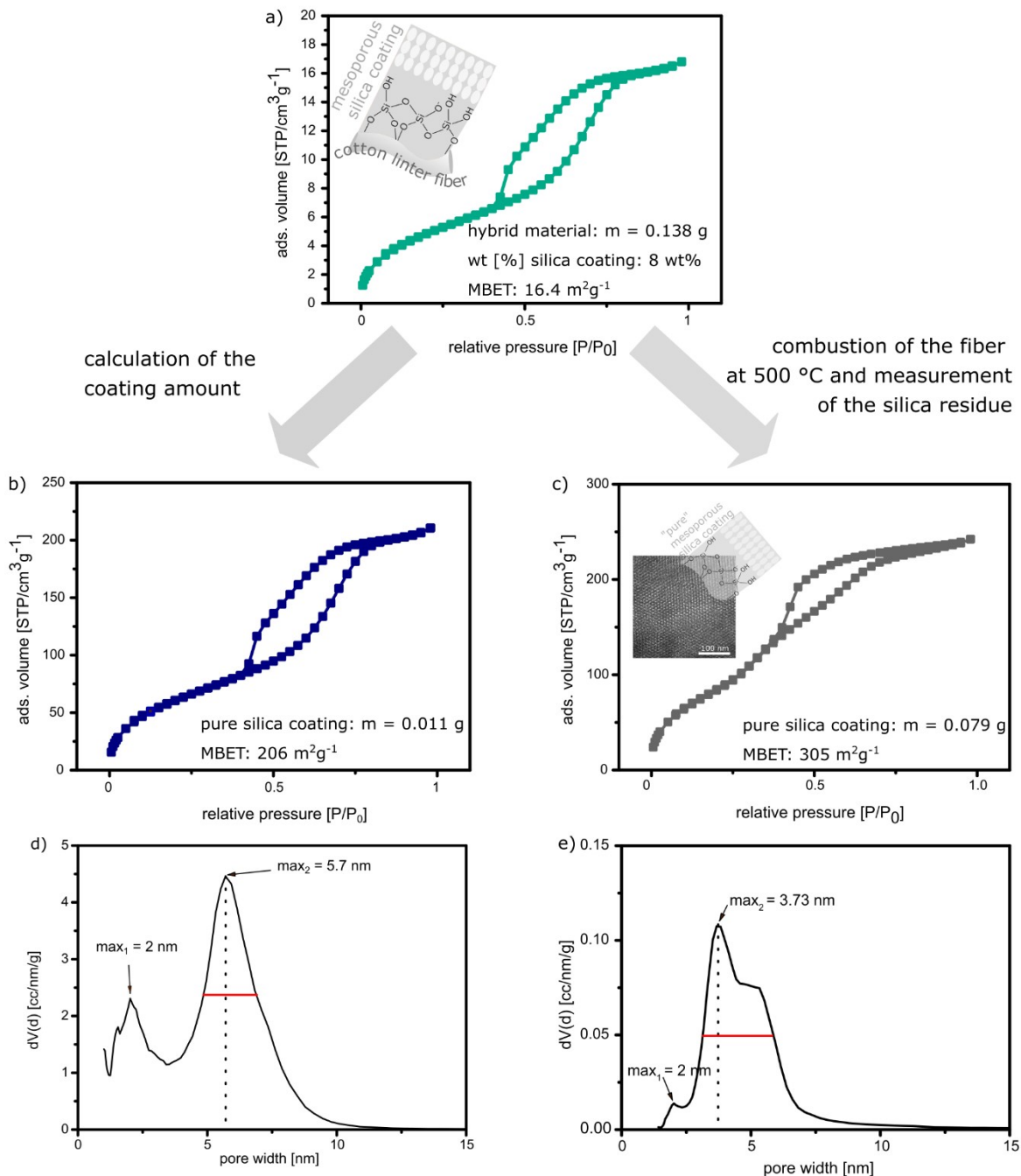


Figure S5: a) Argon 87 K adsorption isotherm of the mesoporous silica coated paper. b) The isotherm of the mesoporous silica coating without paper which is obtained by a sample mass adjustment based on TGA measurements. c) 87 K argon adsorption isotherm of the silica coating after the thermal removal of the cellulose. d) and e) Pore size and pore size distribution of the mesoporous silica coated paper hybrid material (d) and the silica coating after the thermal removal of the cellulose (e) obtained by using a sufficient DFT kernel.

Templating properties of cotton linter papers into silica-based coatings

To prove the templating properties of fibers into silica coatings, a dense silica coating is applied with the standard procedure (experimental details) at cotton linter paper sheets. The sol-gel solution for dense silica coatings do not contain a template which is necessary to form micelles during the coating procedure and with thus for creating pores in the silica coating

(experimental details for sol-gel solution composition). Because of the absence of the template, a dense silica coating without pores is covering the paper fibers. The dense silica coating is covering unevenness of the fiber surface which leads to a smoother surface (see SEM image) and thus a decrease in the specific surface area from $1.2 \text{ m}^2\text{g}^{-1}$ for unmodified papers to $0.72 \text{ m}^2\text{g}^{-1}$. If the coating contains mesopores, the specific surface area would increase because of the introduction of the extra surface through the pores in the coating (Figure 2 a). Cotton linter paper sheets with a mesoporous silica coating have a specific surface area of $16 \text{ m}^2\text{g}^{-1}$ and with this a 13-fold increase in their surface area compared to unmodified papers. Also, the mesopores in the silica coating are detectable with SAXS measurements (Figure S 6 b). Unmodified (black SAXS measurement) and with dense silica coated (orange SAXS measurement) cotton linter paper samples have the same curve shape of the SAXS measurement (Figure S 6 b). The intensity decreases with increasing $q [\text{Å}^{-1}]$ and no positive interference is occurring which would lead to a Bragg peak. SAXS measurements for mesoporous silica coated cotton linter paper show a broad Bragg peak at 0.051 Å^{-1} which indicates scattering centers in mesopore size which are arranged in the distance of 12 nm (Figure S 6 b). After the thermal cellulose paper fiber removal at 500 °C for 2 h the silica coating remains. The result of an argon adsorption measurement is a I b) shaped isotherm with an H 4 hysteresis loop (Figure S 6 c) which indicates the presence of micropores with a wide pore size distribution. Based on a 11-point BET in the relative pressure range of 0.05 to 0.3 a specific surface area of $584 \text{ m}^2\text{g}^{-1}$ has been determined. Compared to the silica-paper hybrid material this is a relative increase of the specific surface area of 834 times. TEM images show the presence of micropores in the dense silica coating after the fiber combustion.

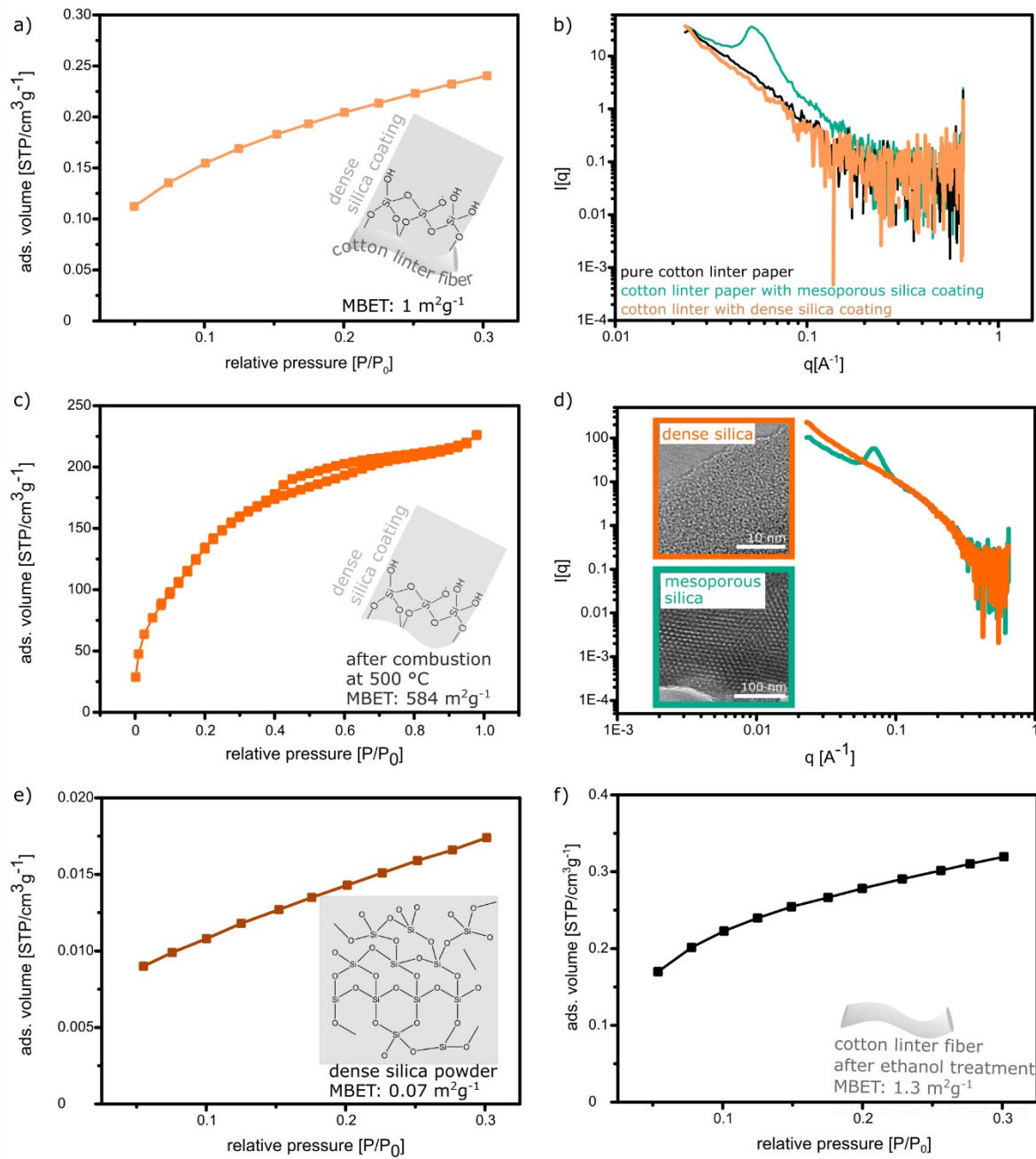


Figure S 6: Krypton 11-point BET at 77 K of dense silica coated cotton linter papers (a), of the dense silica powder (e) and cotton linter fibers after placing them for 3 days in an acidic ethanol solution (f). b) Results of the SAXS measurements from unmodified cotton linter papers (black), cotton linter papers with a dense silica coating (orange) and a mesoporous silica coating (cyan green). c) argon 87 K adsorption isotherm of cotton linter papers with dense silica coating after the thermal removal of the cellulose. d) SAXS measurements of the cotton linter papers with a dense silica coating (orange) and mesoporous silica coating (cyan green) after the thermal removal of the cellulose.

Preparation and silica coating of single cotton linters fibers

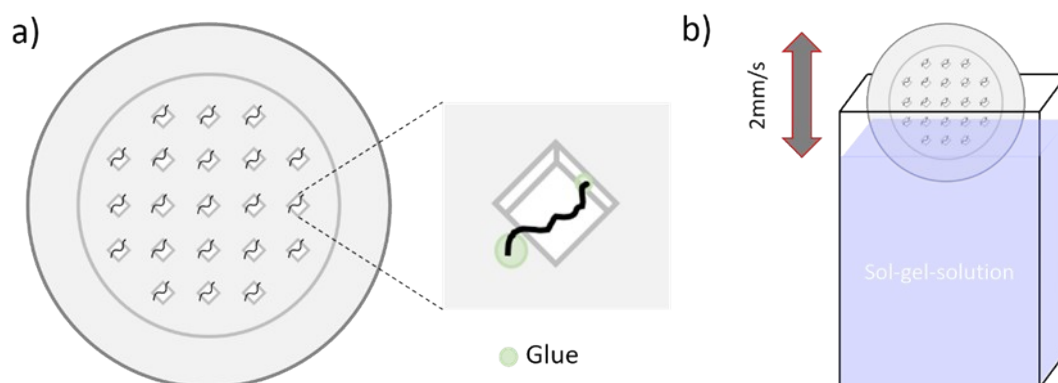


Figure S 7: a) Single fibers mounted on a 3D-printed grid holder with glue. b) schematically depicts the procedure of dip-coating of the mounted fibers.

Selective labelling of silica coating

As an indirect proof for selective fluorescent labelling of silica coatings on single cotton linter fibers, the staining of coated and uncoated fibers was characterized by CLSM imaging. Coated fibers with rhodamine B labelled silica were prepared as described in the experimental section, whereas a comparative reference was realized by incubation of fibers in $4 \cdot 10^{-7}$ M ethanolic rhodamine B solution not containing the silica precursor TEOS. Thermal treatment after staining was applied in analogy to the coating process. Both coated and uncoated fiber types were extracted in DI water for 15 minutes before imaging with CLSM. Figure S 8 depicts the fluorescence microscopic images for both samples, revealing that under identical preparation and imaging conditions the uncoated fibers appear dark with a 10-fold lower average grey value (with respect to the area of the image related to the fiber) compared to the images recorded for the coated fibers. Therefore, it was concluded, that detected fluorescence stems mainly from rhodamine B in the silica coating, while dye adsorption onto uncoated fiber regions results in negligible fluorescence.

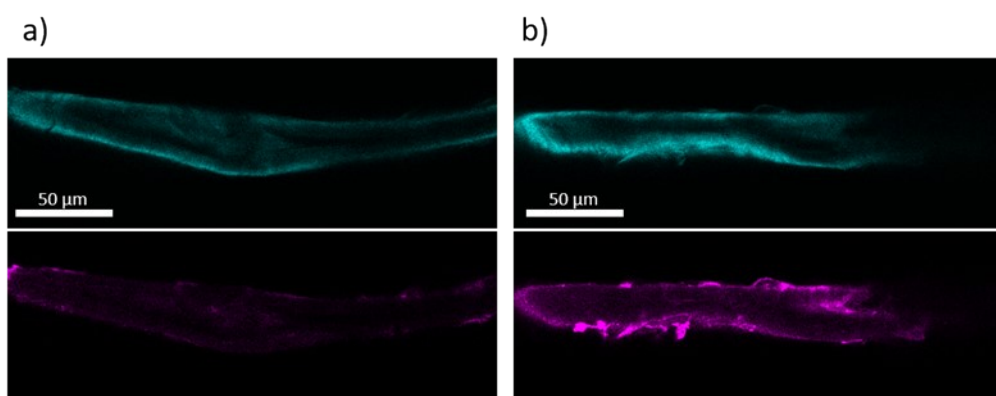


Figure S 8: CLSM images of single cotton linter fibers a) after treatment with rhodamine B solution or b) after dip-coating with rhodamine B containing sol-gel-solution. CFW fluorescence is represented in cyan in the upper images, rhodamine B is illustrated in magenta below.

Localization of silica coatings

By analyzing line profiles within a confocal section of three-dimensional CLSM data (z stacks) of silica coated cotton linter fibers, the relative placement of silica with respect to characteristic fiber structures could be determined. The process of image recording and processing is described in the experimental part, and was applied to a total number of 25 cotton linter fibers. From all recorded z stacks one single optical section is used for the localization of silica coating. Within that optical section, a line profile was drawn perpendicular to the fiber length and the grey values of the different detection channels along the linear profile were compared. The maxima of the profile in the CFW channel were associated with the (inner and outer) fiber walls, while the distance between the two inner maxima is correlated with the fiber lumen. Comparing the profile of rhodamine B channel with the CFW profile finally allows the localization of silica, which can be in general be found in three regions: on the outer and inner fiber walls and inside the lumen of the fiber. Exemplary profiles for each case are presented in Figure S 9.

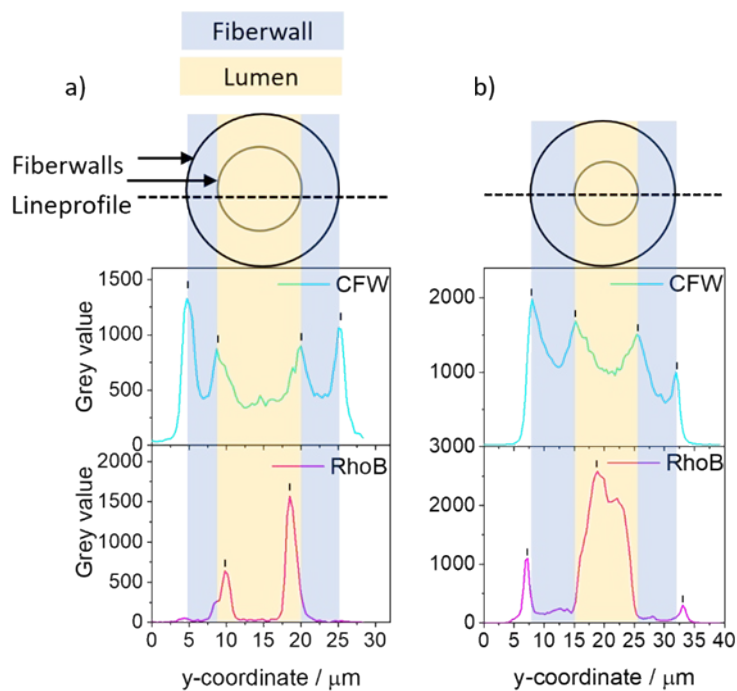


Figure S 9: Line profiles of CFW (cyan) and rhodamine B (magenta) in fluorescence microscopic images of single cotton linter fibers. Peaks in the CFW profiles can be associated with the inner and outer fiber walls. Silica coating could be localized either at the inner fiber walls a), or at the outer fiber walls and in the lumen b).

Differences between cotton linter and eucalyptus sulfate paper

Paper-based materials can be produced either with cellulose or with wood-based fibers. Up to their origin, fibers differ in their structural composition, intrinsic porosity as well as in their morphology. Cotton linter fibers are cellulose based fibers and they are characterized by their high cellulose content, high crystallinity and fiber length. Due to their structural design, the fibers are up to 3 mm long and they have a round shape with a width of up to 50 μm . In the middle of a cotton linter fiber is the fiber lumen located. Compared to cotton linter fibers eucalyptus sulfate fibers are wood based fibers and they are produced via pulping processes

which consist of different chemical steps to remove other wood components such as lignin. The cellulose content is lower and the fibers contain a higher amorphous ratio compared to cotton linter fibers. Based on the fiber origin, eucalyptus sulfate fibers are shorter and flat with a smooth surface. During thermal treatments the fiber structure changes which influences the fiber intrinsic porosity. To create a fiber independent pore structure, mesopores can be introduced in a controlled manner via sol-gel chemistry.

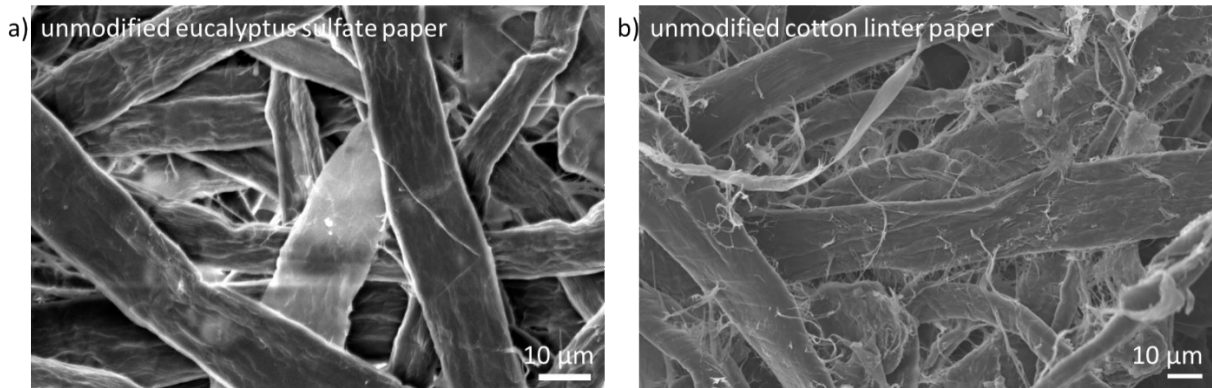


Figure S 10:a) SEM image of unmodified eucalyptus sulfate paper and b) of unmodified cotton linter paper.

Cellulose fiber and paper characterization

Fiber pulp as well as paper specifications for the used cotton linter as well as eucalyptus sulfate fibers/papers before and after silica modification.

Table S 2: Fiber curl, external fibrillation degree, fines content measured with Valmet Fiber Image Analyzer FS5, Valmet Oyi, Espoo, Finland and the drain resistance of the refined cotton linter as well as eucalyptus sulfate fiber pulp. Four measurements were performed with the Valmet Fiber Image Analyzer FS5, whereby the mean value with the standard deviation is shown in the table.

	cotton linter refined ¹ . pulp	eucalyptus sulfate refined ¹ . pulp
fiber curl	14.9 ± 0.2 %	12.5 ± 1.0 %
external fibrillation degree ² .	1.8 ± 0.1 %	1.3 ± 0.0 %
fines content ³ .	17.5 ± 0.6 %	5.3 ± 0.2 %
length-weighted average fiber length	0.95 ± 0.01 mm	0.86 ± 0.00 mm
drainability ⁴ .	23 ± 1°SR	26 ± 2°SR

¹. Laboratory refiner Voith LR 40; Specific Edge Load (SEL): 0.7 Jm⁻¹; Refining Set: 3-1.6-60; Specific Refining Energy: 100 kWh⁻¹

². The fibrillation rate is defined as the ratio between the fibrils area, which are connected to the fiber surface, to the total fiber area, including the main fiber and fibrils, scaled in percent (Laitinen et al. (2014)).

³. Percentage of the length-weighted distribution of particles according to a length smaller than 0.2 mm.

4. Measured using the Shopper Riegler method (ISO 5267-1:1999)

Table S 3: Apparent density, surface roughness and average porosity of unmodified cotton linter and eucalyptus sulfate paper as well as after the mesoporous silica modification.

	cotton linter unmodified paper	cotton linter paper with mesoporous silica coating	eucalyptus sulfate unmodified paper	eucalyptus sulfate with mesoporous silica coating
apparent density ⁶	0.41 gcm ⁻³	0.41 gcm ⁻³	0.55 gcm ⁻³	0.57 gcm ⁻³
surface roughness ⁵	4.8 ± 0.2 μm	4.7 ± 0.4 μm	2.6 ± 0.04 μm	2.7 ± 0.1 μm
average porosity ⁶	72.4 ± 0.5 %	72.9 ± 1.4 %	63.4 ± 0.98 %	61.8 ± 1.8 %

⁵ The paper surface roughness was measured with the Keyence VR-5200, using the arithmetic average of the 3D roughness after ISO 25178-2. An area of 43 mm² of three different samples were used for surface roughness determination and a shape correction of the sample was done for elements larger than 2 mm.

⁶ Apparent density as well as the average porosity is determined using the papers' grammage (1.5 gcm⁻³) and the papers' thickness.

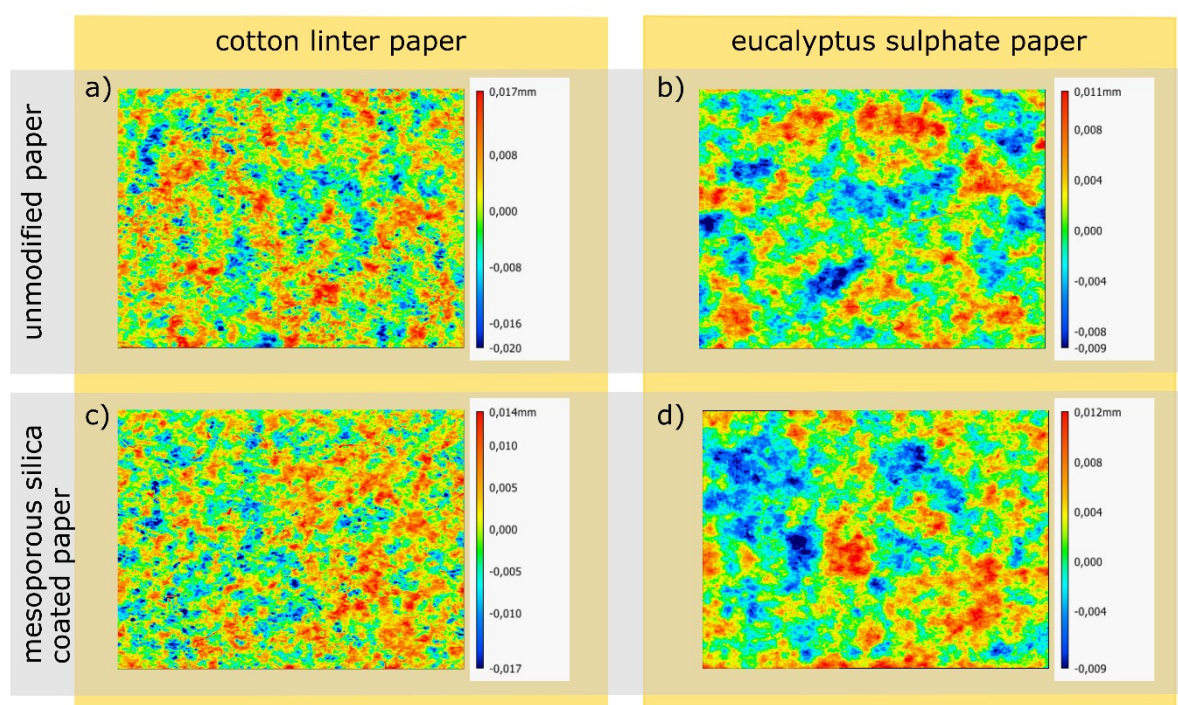


Figure S 11: 43 mm² cutouts of unmodified papers (a cotton linters and b eucalyptus sulphate) and with mesoporous silica coated (c cotton linters and d eucalyptus sulphate) with which the surface roughness was determined using the arithmetic average of the 3D roughness after ISO 25178-2.